Vertical cyclic loading response of a shallow skirted foundation in soft normally consolidated clay

Accepted to Canadian Geotechnical Journal on 12-June-2018

Author 1

- Dimitra Zografou, PhD candidate
- Centre for Offshore Foundation Systems, The University of Western Australia, a node of the ARC Centre of Excellence in Geotechnical Science and Engineering.

Author 2

- Susan Gourvenec, Professor
- Faculty of Engineering and the Environment, University of Southampton, UK. Formerly Centre for Offshore Foundation Systems, The University of Western Australia, a node of the ARC Centre of Excellence in Geotechnical Science and Engineering

Author 3

- Conleth O'Loughlin, Associate Professor
- Centre for Offshore Foundation Systems, The University of Western Australia, a node of the ARC Centre of Excellence in Geotechnical Science and Engineering

Full contact details of corresponding author

- Email: dimitra.zografou@research.uwa.edu.au
- Address: Centre for Offshore Foundation Systems

  The University of Western Australia (M053)

  35 Stirling Highway

  CRAWLEY WA 6009

  Australia

Abstract (200 words)

Skirted foundations are a potential foundation solution for a range of offshore structures including hydrocarbon and renewable energy platforms and subsea structures. Offshore foundations can be subject to cyclic loading from environmental, installation and operational events affecting the geotechnical response. A series of centrifuge tests have been performed on a shallow skirted foundation on normally consolidated kaolin clay under a range of vertical cyclic load sequences, to investigate the effect of tensile or compressive average stress, the magnitude of the applied stress and the effect of cyclic loading of low magnitude followed by consolidation on the foundation response. Results are presented as vertical foundation displacements normalised by the foundation geometry and interpreted within the traditional shear strain contour approach. The findings indicate that the average, rather than maximum, vertical stress defines the foundation vertical displacement response and failure mode; that a threshold stress exists below which a steady state is maintained even at high number of cycles; and that geotechnical resistance increases as a result of low level cyclic loading followed by consolidation.

KEYWORDS: shallow skirted foundations; cyclic loading; centrifuge modelling;

List of notation

CSR	cyclic stress ratio
c_v	vertical coefficient of consolidation
D	diameter
d	skirt depth
d/D	embedment ratio
$D_{T\text{-}bar}$	T-bar diameter
g	standard gravity
G_s	specific gravity
k	undrained shear strength gradient
LL	liquid limit
M	critical state friction constant

N	number of cycles
N_{c0}	bearing capacity factor
N_g	centrifuge acceleration
$N_{T\text{-}bar}$	T-bar capacity factor
PL	plastic limit
q_V	vertical stress
$q_{v,ave}$	average vertical stress
$q_{v,cyc}$	cyclic vertical stress
$q_{v,max}$	maximum (absolute) vertical stress
$q_{V,ult}$	ultimate vertical capacity of foundation
$s_{u\ (consolidated)}$	consolidated soil strength
s_u	undrained shear strength/ monotonic DSS strength
s_{um}	undrained shear strength at mudline
t	dissipation time
T	time factor
t_w	skirt thickness
v	velocity
w	vertical displacement
z	depth
γ_{max}	maximum shear strain
$(\Delta w_{max}/d)\ /\Delta N$	change in normalised maximum vertical displacement per cycle
κ	recompression index
λ	virgin compression index
ν	Poisson's ratio
σ'_v	effective vertical stress
τ_{max}	maximum shear stress

1. Introduction

Skirted foundations are an established foundation type for fixed offshore oil and gas platforms and subsea infrastructure, and more recently for offshore wind turbines (Bye et al. 1995, Watson & Humpheson 2005, Randolph & Gourvenec 2011, Houlsby 2014). The use of shallow skirted foundations, i.e. foundations with a diameter larger than the embedment depth (API 2011), may also offer advantages over deeper foundation options for anchoring vertically tethered platforms (Figure 1). A particular attraction is the potential to resist transient tension if negative excess pore pressures can be generated and maintained between the underside of the foundation base plate and the confined soil plug (House & Randolph 2001, Luke et al. 2005, Gourvenec et al. 2009, Mana et al. 2013), but with lower embedment ratios compared to suction caissons (Tjelta 2001, Tjelta 2015). The larger relative diameter of a shallow foundation compared to a suction caisson provides a significant surface area for ballasting to improve holding capacity that can offset the reduced embedment ratio compared to suction caissons (Gourvenec et al. 2015).

A limited number of research studies have been performed on shallow skirted foundations with low embedment ratios under cyclic loading relevant to floating platforms, although several studies have been performed on the response of suction caissons with embedment ratios higher or equal to 1 (e.g. Andersen et al. 1993, Clukey et al. 1995, Chen & Randolph 2007, Villalobos et al. 2010). The effect of vertical cyclic loading on the (post-cyclic) monotonic capacity of a skirted foundation with embedment ratio of 0.5 on normally consolidated kaolin clay has been investigated with centrifuge testing that indicated a reduction of the monotonic capacity after symmetrical cyclic loading (Byrne & Cassidy 2002). Results from centrifuge tests in carbonate silt of a square shallow skirted foundation, with embedment depth over breadth equal to 0.22, under inclined cyclic load sequences relevant to tension-leg platforms showed that the reverse end bearing capacity can be relied on as long as the loss of embedment is taken into account (Gourvenec et al. 2015). Centrifuge test results of a circular shallow skirted foundations with embedment depth over diameter equal to 0.3 in lightly over-consolidated clay showed an increase in the monotonic undrained uplift capacity after vertical cyclic load sequences, relevant to offloading and refilling of liquefied natural gas terminals, and short consolidation periods

(Acosta-Martinez & Gourvenec 2008). These research studies focus on particular aspects of the foundation response but do not provide a basis for comparison with geotechnical design approaches, nor do they attempt to identify stress thresholds below which the foundation will exhibit a steady response.

The centrifuge experiments that formed the basis of the investigation presented in this paper involved vertical cyclic loading with both average compression and average tensile stresses, and with both low and high maximum load amplitudes. These data provide insight into the stress levels under which a shallow foundation subjected to vertical cyclic loading will respond acceptably from a design perspective. The data also provide a basis for defining the failure criterion based on cyclically degraded strength linked to accumulated strain quantified from strain contour diagrams.

2. Centrifuge experiments

2.1. Experimental arrangement

The centrifuge tests were performed at the National Geotechnical Centrifuge Facility at the Centre for Offshore Foundation Systems in the University of Western Australia using the 1.8 m radius fixed beam centrifuge (Randolph et al. 1991) at an acceleration level of 200 g. The tests involved monotonic and vertical cyclic loading on a circular shallow skirted foundation in normally consolidated kaolin clay. The model foundation had a diameter, D = 60 mm, and a skirt depth, d = 30 mm, giving an embedment ratio, d/D = 0.5, and with a skirt thickness, t_w = 0.48 mm, corresponding in prototype scale to a foundation with a diameter of 12 m, a skirt depth of 6 m and a skirt thickness of 0.096 m. The notation is shown on Figure 1 (b). The model was controlled by the vertical axis of a two-dimensional electrical actuator (see Figure 2). A vent in the top-cap of the foundation allowed the water between the soil surface and the underside of the foundation to be expelled during foundation installation; closing this vent created a seal at the interface of the soil and foundation invert during loading. An ‘S-type’ load cell with a measurement range of 500 N was located directly above the model foundation and allowed the load to be measured in the monotonic tests and controlled during consolidation episodes and in the cyclic tests. Foundation displacement was measured using the optical encoder on the motor of the actuator’s vertical axis.

2.2. Sample preparation and strength profile

The soil sample was prepared by mixing dry kaolin clay with water at twice the liquid limit in a vacuum mixer. The clay properties of the kaolin used at UWA are reported widely; e.g. Stewart (1992), House et al. (2001), Cocjin et al. (2014), and are summarised in Table 1. The kaolin slurry was poured into a sample container, with internal dimensions of 390 mm × 650 mm × 325 mm (width × length × depth), over a 20 mm layer of sand (Figure 2 (b)), such that there was two-way drainage of the sample. Geotextile drains were also placed at the corners of the sample to provide a hydraulic connection between the base and top of the sample. A 40 mm water layer was maintained on the sample surface during consolidation and over the course of the testing to ensure sample saturation. The soil sample was consolidated initially in the centrifuge at 200 g for 3.5 days. After consolidation, the surface of the sample was scraped level at 1g (noting that in-flight consolidation creates a curved sample surface), removing < 1 mm of clay at the middle of the sample and approximately 10 mm at the sample edges, to ensure that the skirts of the foundation 'touched-down' on the sample surface at the same time. The sample was then spun back to 200 g for a further day before starting the sample characterisation tests.

Three T-bar tests were carried out to determine the undrained shear strength profile, s_u, of the soil sample before testing using a model scale T-bar penetrometer with a diameter, $D_{T\text{-}bar}$ = 5 mm. The T-bar tests employed a penetration velocity, v = 1 mm/s, such that the dimensionless ratio, $D_{T\text{-}bar}.v/c_v$ > 30 and undrained conditions were achieved (Finnie & Randolph 1994) (c_v is the vertical coefficient of consolidation based on one-dimensional Rowe cell consolidation test data on kaolin clay, House et al, (2001), Cocjin et al. (2014) - see Table 1). Each T-bar test involved an episode of cyclic remoulding, in which the T-bar was moved vertically up and down over four T-bar diameters at v = 1 mm/s for ten cycles to remould the clay. This allowed the measured T-bar penetration resistance to be corrected for soil buoyancy, weight changes of the load-cell and T-bar probe (due to the changing centrifuge acceleration with radius) and lateral stresses from the soil on the load cell gauges (Sahdi et al. 2014). The cyclic remoulding phase of the T-bar tests was carried out between depths of 40 mm and 60 mm, sufficiently deep to avoid entrainment of surface water, within the region of interest of the tests but not too close to the foundation skirt depth. The undrained shear strength, s_u, was derived from the corrected

penetration resistance using the commonly adopted T-bar capacity factor $N_{T\text{-}bar}$ = 10.5 (Martin & Randolph 2006) and the resulting profile of s_u with penetration depth, z (in prototype scale) is provided in Figure 3, with the idealised profile, $s_u = s_{um} + kz$, where s_{um} is the undrained shear strength at the mudline, $s_{um} \sim 0$ kPa, and k is the undrained shear strength gradient, k ~ 0.90 kPa/m.

2.3. Foundation Installation Procedure

The foundation was installed with the drainage vent open at a velocity, v = 0.1 mm/s such that the system response is undrained ($D.v/c_v$ = 82), although some local consolidation near the skirt tips may have occurred ($t_w.v/c_v$ = 0.7). Installation penetration was halted at touchdown of the underside of the foundation, confirmed by a sharp increase in the installation resistance. The centrifuge was then spun down so that the vent could be sealed and spun up again prior to the foundation load test. Before the commencement of the monotonic test, a compressive vertical stress equal to the installation resistance was applied on the foundation for a period of 788 s (1 year in prototype scale). The installation resistance was equal to ~16% of the ultimate monotonic vertical capacity, defined retrospectively from the monotonic test. In the cyclic tests, a vertical stress equal to 20% of the ultimate monotonic vertical capacity was applied after the installation resistance to represent the submerged weight of the foundation and was held for a period of 788 s (1 year in prototype scale) prior to application of the vertical load cycles, to ensure all tests started from a similar effective stress state. The degree of consolidation associated with this waiting period is estimated as approximately 10% based on the assumption of a smooth skirt (Gourvenec & Randolph 2010).

2.4. Experimental programme

As part of this study, a vertical monotonic test and five vertical cyclic tests were carried out. The monotonic test was carried out under displacement control at v = 0.1 mm/s (such that the response was undrained, $D.v/c_v$ = 82) to define the ultimate undrained monotonic vertical capacity, $q_{V,ult}$. The cyclic tests were performed under load control and the vertical stress, q_v, that is the applied vertical load divided by the foundation base area, was applied as a percentage of $q_{V,ult}$. Details of the cyclic tests and their purpose are provided in Table 2 and a schematic representation of the loading sequences is shown on Figure 4 (a) to (e). It is noted that in this study, compressive vertical stress and

downward vertical displacement are considered positive, as illustrated in Figure 1 (b), while tensile vertical stress and upwards vertical displacement are considered negative. The vertical stress in the cyclic tests comprises the average vertical stress, $q_{V,ave}$, and the cyclic vertical stress, $q_{V,cyc}$. The components of average and cyclic vertical stress along with the maximum (absolute) value of vertical stress, $q_{v,max}$, are illustrated on Figure 4 (c).

The cyclic tests involved vertical non-symmetrical, two-way cyclic loading applied in the form of sinusoidal waves at a frequency of 0.25 Hz. The parcels of uniform vertical stress applied in the cyclic tests comprised 1080 cycles, corresponding to the number of cycles in a typical 3-hour storm, unless failure was reached before the end of the sequence. The loading frequency was selected to ensure the response was undrained in each loading cycle, whilst ensuring the quality of load control.

Two cyclic staged tests were carried out with parcels of uniform vertical stress with magnitudes in ascending order; the first staged test with parcels in average tension (except for the first three parcels) [ASC_TENS] and the second staged test with parcels in average compression [ASC_COMP]. The staged tests in average tension and in average compression were chosen to represent potential cyclic load conditions for tethered platforms during a storm, although both sequences are highly idealised. Three cyclic tests with uniform amplitude in average tension were also carried out; a test with a relatively high tensile vertical stress ($q_{Vmax} = -0.8\ q_{V,ult}$) [HIGH] and two tests with relatively low tensile vertical stress ($q_{V,max} \approx -0.4\ q_{V,ult}$) followed by a consolidation period [LOW-CONS and LOW_CONS_HIGH]. The aim of these uniform tests was to investigate the foundation response under a range of applied loads and the effect of low-magnitude cyclic loading, relevant to calm weather environmental loading, on the soil and foundation response.

3. Centrifuge test results

3.1. Comparison of foundation response under cyclic loading in average compression and average tension

Figure 5 shows a comparison of the response of the skirted foundation in the staged cyclic tests with parcels in average tension [ASC_TENS] and in average compression [ASC_COMP]. The data on

Figure 5 are presented in terms of the vertical displacement, w, normalised by the foundation skirt depth, d, and the change in normalised maximum vertical displacement per cycle, $(\Delta w_{max}/d)/\Delta N$, where w_{max} is the maximum vertical displacement in a cycle. Figure 5 shows that under average tension, the foundation displaced upwards (noting that the first two parcels of ASC_TENS were in compression). The rate of displacement, given by $(\Delta w_{max}/d)/\Delta N$, was essentially constant until N = 17096 in the last parcel when $(\Delta w_{max}/d)/\Delta N$ started to increase suddenly. At this point, suction between the underside of the base plate and the confined soil plug was lost, resulting in the foundation being pulled out rapidly. Under average compressive load, the foundation displaced downwards continously and the rate of displacement $(\Delta w_{max}/d)/\Delta N$ remained constant and generally lower than 0.2% throughout the test. These results are consistent with other published findings that the direction of vertical displacement of a skirted foundation depends on the average vertical stress rather than the maximum vertical stress (Bye et al. 1995, Byrne & Houlsby 2002, Kelly et al. 2006, Randolph 2012).

Based on the above, the average vertical stress appears to define the foundation vertical displacement response and failure mode. Catastrophic failure eventually occurred in the test with parcels in average tension while no instability failure was observed in the test with parcels in average compression. As a result, it was decided that the rest of the cyclic test programme would consider only sequences in average tension, while acknowledging the importance of failure defined by a prescribed magnitude of displacement, including settlement, for a serviceability limit state.

3.2. Stable and unstable vertical displacement response in cyclic uniform tests in average tension

Figure 6 (a) presents the vertical displacement in three uniform cyclic load tests in average tension with relatively high cyclic stress $(q_{V,ave} \pm q_{V,cyc})/q_{V,ult}$ = -0.30 ± 0.50 [HIGH] and relatively low stress $(q_{V,ave} \pm q_{V,cyc})/q_{V,ult}$ = -0.10 ± 0.30 [LOW_CONS and LOW_CONS_HIGH] in the first 12 cycles. Figure 6 (b) shows the vertical displacement response over the duration of the first parcel of cyclic loading in the two low stress level tests. Figure 6 (a) shows that the vertical displacement response became unstable early in the test at high stress level, with both the average and cyclic components of vertical displacement increasing, while the vertical displacement remained stable in the tests under low stress.

Figure 6 (b) shows that the response under low stress remained stable throughout the entire parcel of cyclic loading, i.e. over N = 1080 cycles. It is noted that some background consolidation may be taking place during the cyclic loading in these tests, as discussed later in the paper, but it is not considered to affect the vertical displacement response as the applied loading and foundation response was stable consistently from the onset of cyclic loading. The difference in the response in the tests presented in Figure 6 (a) – i.e. unstable response with N < 10 under high stress and stable response with N > 1000 in the tests under low stress – indicate the existence of a threshold stress, below which a stable response can be anticipated irrespective of the duration of loading, or number of cycles. This is consistent with observations from field tests on piles under axial cyclic loading, that indicate a combination of average and cyclic loads that lead to a stable response of axial displacement for a high number of cycles (Jardine et al. 2012, Jardine & Standing 2012, Tsuha et al. 2012, Rimoy et al. 2013). A stable vertical displacement response has been also observed in model tests on a suction caisson with d/D = 6 in normally consolidated clay under low symmetrical tensile cyclic loading for over 10000 cycles (Iskander et al. 2002). In the current study, it appears that there may be a threshold value, or a combination of values of $q_{V,ave}/q_{V,ult}$ and $q_{V,cyc}/q_{V,ult}$ that lead to a stable vertical displacement response for cyclic loading with N > 1000. Based on the centrifuge tests under two-way cyclic loading in average tension, the threshold between stable and unstable response lies between $(q_{V,ave} \pm q_{V,cyc})/q_{V,ult}$ = -0.10 ± 0.30 and -0.30 ± 0.50 for the conditions considered.

3.3. Effect of low-magnitude cyclic loading and consolidation on foundation response

Figure 7 compares the foundation response in the uniform test with $(q_{V,ave} \pm q_{V,cyc})/q_{V,ult}$ = -0.30 ± 0.50 [HIGH] (a and c) with the test with uniform cyclic loading followed by a consolidation period and a parcel of cyclic loading of high magnitude [LOW_CONS_HIGH] (b and d). Loss of suction, and therefore instability failure, occurred when $(\Delta w_{max}/d)/\Delta N$ increased rapidly, which was after 7 cycles in the test with high average stress (Figure 7c) and after 41 cycles in the test preceded by low-level cyclic loading (Figure 7d). As loss of suction occurred in test LOW_CONS_HIGH at a higher number of cycles than in test HIGH and at a slightly higher value of applied vertical stresses, it appears that the geotechnical resistance increased with time due to the parcel of cyclic loading at lower magnitude and

consolidation. Loss of suction occurred at similar levels of vertical displacement in the tests, with w_{max}/d equal to approximately 5.9% and 5.2% in tests HIGH and LOW_CONS_HIGH respectively.

Dissipation of excess pore water pressure, inside and around the skirts of the foundation, takes place faster in the centrifuge than in the field as consolidation times are scaled by N_g^2, where N_g is the centrifuge acceleration (Garnier et al. 2007). Therefore, while cyclic loading can be carried out at a frequency to ensure undrained conditions during a single cycle, a greater degree of consolidation will occur in the centrifuge during a period of cyclic loading than would take place in the equivalent field situation. Dissipation of the excess pore water pressure during cyclic loading in these centrifuge tests is referred to here as background consolidation. The degree of background consolidation can be quantified by the dimensionless time factor, T defined as

$$T = c_V . \frac{t}{D^2} \qquad (1)$$

where c_v is the vertical coefficient of consolidation quantified in Table 1, t is the dissipation time, and D is the foundation diameter as defined earlier. Figure 8 presents the vertical displacement response in cyclic tests LOW_CONS and LOW_CONS_HIGH as a function of both t (prototype scale) and T, where the origin of time is taken as the application of the monotonic vertical 'self-weight' stress at the start of the test. Figure 8 shows that the vertical displacement of the foundation under the monotonic vertical stress appears to stabilise by the end of the consolidation period, indicating that consolidation is essentially complete during the period after the first cyclic parcel. The degree of consolidation, U, can be approximated from numerical solutions for vertically loaded circular skirted foundations (Gourvenec & Randolph 2010). For test LOW_CONS_HIGH, T = 0.14 for the 1080 cycles in the first cyclic parcel corresponds to U ≈ 30%, T = 0.54 at the end of the consolidation period corresponds to U ≈ 70%, while T = 0.04 for the 41 cycles in the second cyclic parcel corresponds to U ≈ 5%. This indicates that some degree of background consolidation occurred in the first parcel, while almost complete dissipation of the excess pore water pressure occurred during the consolidation period after the first cyclic parcel and essentially no background consolidation occurred in the second cyclic parcel. The increase in net geotechnical resistance in test LOW_CONS_HIGH noted above, can be therefore

attributed to the dissipation of excess pore water pressure induced by the cyclic load parcel and by the constant vertical stress that was maintained before and after the cyclic parcel.

To assess the effect of the low-magnitude cyclic loading and consolidation on the undrained shear strength, s_u, T-bar tests were performed through the test footprint of test LOW_CONS (that comprised a parcel of low amplitude loading and a consolidation period similar to LOW_CONS_HIGH), and at an undisturbed location in the sample both before testing and after the completion of testing (four days after completion of the cyclic test). The s_u profiles are provided in Figure 9, which shows that marginal change in undrained shear strength occurred in the undisturbed sample during the testing period, reinforcing the previous observation that consolidation of the soil sample had been achieved prior to testing. However, Figure 9 does show that s_u is higher at the test location than at undisturbed locations after completion of testing, both over the depth of the skirts and below skirt tip level. The increase is almost 70% at the edge of the foundation footprint at skirt tip level, but a more moderate 20% in the centre of the foundation footprint.

Based on the above, a gain in s_u, and therefore in the net geotechnical resistance, is achieved if full consolidation occurs after low-magnitude cyclic loading. Similar to observations from this study, previous experimental studies have shown that cyclic displacements or cyclic loading on model riser pipes on soft normally or lightly overconsolidated clay may lead to an increase of the undrained shear strength of the underlying soil, if adequate dissipation of the excess pore water pressure is allowed after the remoulding of the soil (Hodder et al. 2013, Yuan et al. 2015, Clukey et al. 2017, Cocjin et al. 2017) and that the undrained sliding of a shallow foundation followed by adequate consolidation may cause enhancement of the foundation monotonic vertical capacity and sliding resistance respectively (Cocjin et al. 2014). In these examples the cyclically induced gains are greater than under equivalent monotonic loading. While it is impractical to rely on these strength gains in initial design – since the timing of the design event is unknown – insight into consolidation gains from a lifetime of calm weather cyclic loading can inform on foundation stability for life extension design or decommissioning.

4. Failure criteria on a shear strain contour diagram

Strain accumulation on contour diagrams is a well-established approach for geotechnical design of foundations under cyclic loading by assessing soil strength degradation due to cyclic loading. The approach converts real irregular cyclic load sequences to an idealised regular cyclic load sequence through an accumulation procedure on contour diagrams of shear strain or excess pore water pressure based on results from laboratory element tests (Andersen 2015). The contour with the highest value is considered the failure envelope and the stress level where the accumulation procedure intersects the failure envelope is defined as the cyclic shear strength that determines the foundation cyclic capacity.

This section attempts to define appropriate failure criteria for vertical cyclic loading of a shallow foundation by associating the failure envelope on a contour diagram, derived from element tests, with the instability failure observed in the centrifuge tests. A shear strain contour diagram derived from stress-controlled cyclic non-symmetrical direct simple shear (DSS) tests (with $\tau_{ave} = \tau_{cyc}$, where τ_{ave} is the average shear stress and τ_{cyc} is the cyclic shear stress) on normally consolidated kaolin clay, the same material used in the centrifuge tests, is adopted. The test details are presented by Zografou et al. (2018a) and the contour diagram with cyclic stress ratio, CSR, ($= \frac{\tau_{cyc}}{\tau_{ave}}$) of 1 is shown on Figure 10. The contours of maximum shear strain, γ_{max}, are presented as a function of maximum shear stress, τ_{max}, normalised by the monotonic DSS strength, s_u. The DSS tests used to develop the contour diagram are considered relevant here as DSS strength can be considered as an average strength between triaxial compression and triaxial extension (Mayne 1985, Randolph 2012). The DSS strength is considered representative of the range of stress paths in the soil surrounding and beneath a shallow foundation and therefore of the soil strength mobilised by a foundation at failure. The comparison of the foundation response in the centrifuge with the soil response under DSS is made based on the assumption that the ratio of normalised vertical stress, $q_{V,max}/q_{V,ult}$ is equal to the ratio of normalised shear stress, τ_{max}/s_u applied on a soil element. It is noted that the ratio $q_{V,cyc}/q_{V,ave}$ in the centrifuge tests considered below (HIGH and last parcel of LOW_CONS_HIGH) varies from 0.7 to 1.6 (Table 2), and is therefore close to the value of CSR = 1 in the cyclic DSS tests.

The failure envelope on the contour diagram can be defined as the contour that is closest to the final point of the accumulation procedure for the centrifuge tests that reached failure. As discussed previously, instability failure occurred in the cyclic tests under average tension when suction was lost. In the centrifuge test with a single parcel of high cyclic loading, the 'instability failure' envelope on the contour diagram of shear strain can be defined as the contour that corresponds to the normalised shear stress and number of cycles where loss of suction was observed. Loss of suction in the test with high average vertical stress was observed at $q_{V,max}/q_{V,ult}$ = -0.8 and N = 7. Figure 10 shows that the contour that corresponds to loss of suction in this test is the contour of γ_{max} = 5%, at $\tau_{max}/s_{u\ (consolidated)}$ = -0.76 and N = 7. Consolidated soil strength, $s_{u\ (consolidated)}$ is considered here to account for the increase in s_u during the waiting period under the monotonic vertical stress. The value of $s_{u\ (consolidated)}$ is estimated based on a theoretical framework, verified by back-calculating s_u values from uplift resistance in centrifuge uplift tests of a shallow skirted foundation (d/D = 0.2) in lightly over-consolidated kaolin clay following preloading and consolidation (Li et al. 2015), and numerical results reported by Vulpe et al. (2017) for a monotonic vertical stress $q_V/q_{V,ult}$ = 0.2 and T = 0.04 (Figure 8).

The normalised shear stress and number of cycles at failure are also plotted on the contour diagram on Figure 10 for the centrifuge test with low-level cyclic loading followed by a consolidation period and a parcel of cyclic loading of high magnitude [LOW_CONS_HIGH] ($q_{V,max}/q_{V,ult}$ = -0.95 and N = 41). It is noted that the first parcel with $q_{V,max}/q_{V,ult}$ = -0.36 (-0.10 ± 0.30) and N = 1080 plots near the horizontal contour of 1% and is not considered in the accumulation procedure (Zografou et al. 2018a, Zografou et al. 2018b). As shown in Figure 9 and discussed above, T-bar tests through the foundation footprint in the cyclic test with the same sequence until the end of consolidation period [LOW_CONS indicated that the increase in s_u is between 20%, close to the centre of the foundation and up to 70% close to the edges of the foundation. Assuming an increase in operative s_u of 45%, Figure 10 shows that loss of suction in the test LOW_CONS_HIGH plots at the contour of γ_{max} = 5%, at $\tau_{max}/s_{u\ (consolidated)}$ = -0.66 and N = 41.

Based on the above, a shear strain of γ_{max} = 5% in a soil element under cyclic DSS may be linked with instability failure of the shallow skirted foundation in normally consolidated kaolin clay under the cyclic

sequences tested in the centrifuge. This value of γ_{max} is below the contour where failure at a soil element level was defined, i.e. γ_{max} = 25% - also shown on Figure 10 and defined in the same way as failure for the model tests reported here, i.e. at the point where the change in γ_{max} per cycle increases rapidly (Zografou et al. 2018a). The findings indicate that instability failure of the foundation under tension occurred at a common strain level irrespective of loading history, although the strain level is not immediately comparable to that defining failure at the element level in the DSS tests.

5. Conclusions

This paper presents results from centrifuge tests on a shallow skirted foundation in normally consolidated kaolin clay under two-way non-symmetrical vertical cyclic loading. Based on the observations from the centrifuge tests, the following conclusions can be made:

1. Two-way cyclic loading in average compression leads to continuous accumulation of the vertical settlement of the foundation while two-way cyclic loading in average tension may lead to a loss of embedment, leading to loss of passive suction and an instability failure. The mode of failure for a skirted foundation under two-way vertical cyclic loading therefore appears to depend on the average vertical stress, rather than the maximum. Based on the present study, suction was lost when upward vertical displacement was approximately 5% of the embedment depth. In addition, it was observed that cyclic loading in average compression led to higher magnitude of vertical displacement than cyclic loading in average tension of similar magnitude.
2. A threshold value of applied vertical stress was observed below which the vertical displacement remained stable for a high number of cycles. Vertical displacement was stable under cyclic loading in average tension for > 1000 cycles with a relatively low normalized vertical stress $(q_{V,ave} \pm q_{V,cyc})/q_{V,ult}$ = -0.10 ± 0.30 while an unstable response was observed at N < 10 with a higher amplitude cyclic stress $(q_{V,ave} \pm q_{V,cyc})/q_{V,ult}$ = -0.30 ± 0.50. Generalised conclusions regarding threshold stresses for skirted foundations cannot be drawn from the limited data from this test program. The observation that a threshold stress combination exists is potentially significant, and investigation of a wider range of foundation, soil and loading conditions would be of value, as threshold stress is an important consideration in foundation design.

3. Two-way cyclic loading in average tension of low magnitude stresses followed by a consolidation period has been shown to increase soil strength, evidenced by the higher maximum stress and relatively high number of cycles at which failure occurred.
4. The instability failure envelope of the cyclic centrifuge tests in average tension, plotted on a shear strain contour diagram derived from cyclic direct simple shear test data, was defined on a shear strain contour (γ_{max} = 5%) that is notably lower than the maximum shear strain where failure was observed in the element tests on the same soil.

Acknowledgements

This work forms part of the activities of the Centre for Offshore Foundation Systems (COFS). Established in 1997 under the Australian Research Council's Special Research Centres Program. Supported as a node of the Australian Research Council's Centre of Excellence for Geotechnical Science and Engineering, and through the Fugro Chair in Geotechnics, the Lloyd's Register Foundation Chair and Centre of Excellence in Offshore Foundations and the Shell EMI Chair in Offshore Engineering. The work presented in this paper was supported through ARC grant CE110001009. This support is gratefully acknowledged.

Table captions

Table 1 Typical properties of kaolin clay

Table 2 Overview of centrifuge tests

Figure captions

Figure 1 (a) A tension-leg platform anchored with skirted foundations and (b) skirted foundation geometry (with sign convention for vertical stress, q_v, and vertical displacement, w, used in the model tests)

Figure 2 Experimental arrangement: (a) photograph and (b) schematic representation

Figure 3 Undrained shear strength profile

Figure 4 Schematic representation of the applied vertical cyclic stress sequences in the cyclic centrifuge tests: (a) staged cyclic test in average tension (except in the first two parcels) with parcels of uniform cyclic loading increasing in magnitude in ascending order [ASC_TENS], (b) staged cyclic test in average compression with parcels of uniform cyclic loading with magnitude increasing in ascending order [ASC_COMP], (c) uniform cyclic test in average tension and high magnitude [HIGH], (d) cyclic test (in average tension) with a parcel of uniform cyclic loading of relatively low magnitude followed by a consolidation period and a parcel of uniform cyclic loading of high magnitude [LOW_CONS_HIGH] and (e) cyclic test with a parcel of uniform cyclic loading of relatively low magnitude followed by a consolidation period [LOW_CONS]

Figure 5 Vertical displacement history (vertical displacement normalised by embedment depth) during cyclic loading for (a) staged cyclic test in average compression [ASC_COMP], (b) in average tension [ASC_TENS], and c) change of vertical displacement per cycle in test ASC_COMP and d) near failure in test ASC_TENS

Figure 6 (a) Vertical displacement history for cyclic test with uniform high tensile vertical stress [HIGH] and tests with parcel of low tensile vertical stress [LOW_CONS, LOW_CONS_HIGH] over the first 12 cycles and (b) in a parcel of low tensile vertical stress [LOW_CONS, LOW_CONS_HIGH] over 1080 cycles.

Figure 7 Vertical displacement history for (a) cyclic test with uniform high tensile vertical stress [HIGH]; N = 0 - 12, and (b) cyclic test with uniform cyclic loading in average tension followed by a consolidation period and a parcel of cyclic loading of high magnitude, in the second parcel [LOW_CON_HIGH]; N = 0 - 50, and (c, d) change in w_{max} per cycle

Figure 8 Vertical displacement response under a monotonic vertical stress of $0.2q_{V,ult}$ before and after cyclic loading [LOW_CONS] as a function of time, t, and as a function of dimensionless time factor, T.

Figure 9 Profiles of undrained shear strength before and after testing

Figure 10 Final points of accumulation procedure for centrifuge test with high tensile vertical stress [HIGH] and with low-level cyclic loading followed by consolidation and then parcel with high tensile vertical stress [LOW_CONS_HIGH] on a contour diagram of maximum shear strain based on cyclic DSS tests (CSR = 1) on normally consolidated kaolin clay by Zografou et al. (2018a)

6. References

Acosta-Martinez, H.E. & Gourvenec, S.M. (2008). Response of skirted foundations for buoyant facilities subjected to cyclic uplift loading. In Proceedings of The Eighteenth International Offshore and Polar Engineering Conference. International Society of Offshore and Polar Engineers, Vancouver, Canada, 705-712.

Andersen K.H. (2015). Cyclic soil parameters for offshore foundation design, In Proceedings of the Frontiers in Offshore Geotechnics III, Oslo, Norway, 5-82

Andersen, K.H., Dyvik, R., Schrøder, K., Hansteen, O.E., & Bysveen, S. (1993). Field tests of anchors in clay. II: Predictions and interpretation. Journal of Geotechnical Engineering, 119 (10): 1532–1549

API RP 2GEO (2011). Recommended Practice for Geotechnical Foundation Design Consideration.

Bye, A., Erbrich, C., Rognlien, B. & Tjelta, T.I. (1995) Geotechnical design of bucket foundations. In Proceedings of the 27th Offshore Technology Conference., Houston, USA, 869–883.

Byrne B.W. & Houlsby, G.T. (2002). Experimental investigations of response of suction caissons to transient vertical loading. Journal of Geotechnical and Geoenvironmental Engineering, 128 (11), 926-939.

Byrne, B.W. & Cassidy, M.J. (2002). Investigating the response of offshore foundations in soft clay soils. In ASME 2002 21st International Conference on Offshore Mechanics and Arctic Engineering, 263-275. American Society of Mechanical Engineers.

Chen, W. & Randolph, M.F., (2007). Uplift capacity of suction caissons under sustained and cyclic loading in soft clay. Journal of Geotechnical and Geoenvironmental Engineering, 133 (11), 1352-1363.

Clukey E.C., Morrison M. J., Garnier J. & Corte J.F (1995). The response of suction caissons in normally consolidated clays to cyclic TLP loading conditions. Offshore technology conference, Houston, Texas, OTC 7796

Clukey, E. C., Aubeny, C. P., Zakeri, A., Randolph, M. F., Sharma, P. P., White, D. J., Sancio R. & Cerkovnik, M. (2017). A Perspective on the State of Knowledge Regarding Soil-Pipe Interaction for SCR Fatigue Assessments. Offshore Technology Conference, OTC-27564-MS

Cocjin M.L, Gourvenec S.M, White D.J. & Randolph M.F. (2014). Tolerably mobile subsea foundations – observations of performance. Geotechnique, 64 (11) 895–909.

Cocjin, M.L., Gourvenec, S.M., White, D.J. & Randolph, M.F., 2017. Theoretical framework for predicting the response of tolerably mobile subsea installations. Géotechnique, 67 (7), 608-620

Finnie, I.M.S. & Randolph, M.F. (1994). Punch-through and liquefaction induced failure of shallow foundations on calcareous sediments. In Proceedings of the International Conference on Behavior of Offshore Structures, BOSS ’94, Boston, 4–7 July 1994, 217–230.

Garnier J., Gaudin C., Springman S.M., Culligan P.J., Goodings D., Konig D., Kutter B., Phillips R., Randolph M.F. & Thorel L. (2007). Catalogue of scaling laws and similitude questions in geotechnical centrifuge modelling. International Journal of Physical Modelling in Geotechnics, 7 (3), 1-23.

Gourvenec S.M., Neubecker S., Senders M., & White D.J. (2015). Performance of a shallow skirted foundation for TLP mooring in carbonate silt, Frontiers in Offshore Geotechnics III: proceedings of the Third International Symposium on Frontiers in Offshore Geotechnics (ISFOG 2015), Oslo, Norway, 10-12 June 2015, CRC Press, Boca Raton, 257-262

Gourvenec, S. & Randolph, M.F., (2010). Consolidation beneath circular skirted foundations. International Journal of Geomechanics, 10 (1), 22-29.

Gourvenec, S., Acosta-Martinez, H.E. & Randolph, M.F., (2009). Experimental study of uplift resistance of shallow skirted foundations in clay under transient and sustained concentric loading. Géotechnique, 59(6), 525-537.

Hodder M.S., White D.J. & Cassidy M.J. (2013) An effective stress framework for the variation in penetration resistance due to episodes of remoulding and reconsolidation. Geotechnique 63 (1), 30–43

Houlsby (2014). Houlsby, G., 2016. Interactions in offshore foundation design. Rankine Lecture.

House, A.R. & Randolph, M.F., (2001). Installation and pull-out capacity of stiffened suction caissons in cohesive sediments. In The Eleventh International Offshore and Polar Engineering Conference. International Society of Offshore and Polar Engineers.

House A., Oliveira J.R.M.S. and Randolph M.F. (2001). Evaluating the coefficient of consolidation using penetration tests. *International Journal of Physical Modelling in Geotechnics*, 1(3): 17–26.

Iskander M., El-Gharbawy S. & Olson R. (2002). Performance of suction caissons in sand and clay. Canadian Geotechnical Journal, 2002, 39(3): 576-584

Jardine R.J & Standing J.R. (2012), Field axial cyclic loading experiments on piles driven in sand, Soils and Foundations, 52 (4), 723-736.

Jardine R.J., Andersen, K. & Puech, A. (2012). Cyclic loading of offshore piles: potential effects and practical design. In Proceedings of the 7th International Conference on Offshore Site Investigations and Geotechnics, Society for Underwater Technology, London, 59-100.

Kelly, R.B., Houlsby, G.T. & Byrne, B.W., (2006). Transient vertical loading of model suction caissons in a pressure chamber. Geotechnique 56, No. 10, 665–675

Li, X., Gaudin, C., Tian, Y. & Cassidy, M.J., (2015). Effects of preloading and consolidation on the uplift capacity of skirted foundations. Géotechnique, 65 (12), 1010-1022.

Luke A.M., Rauch A.F., Olson R.E. & Mecham E.C. (2005). Components of suction caisson capacity measured in axial pullout tests. Ocean Engineering, 32 (7), 878-891.

Mana D.S.K., Gourvenec S.M. & Randolph M.F. (2013). Experimental investigation of reverse end bearing of offshore shallow foundations. Canadian Geotechnical Journal, 2013, 50 (10), 1022-1033

Martin, C.M. & Randolph, M.F., (2006). Upper-bound analysis of lateral pile capacity in cohesive soil. Géotechnique, 56 (2), 141-145.

Mayne, P.W. (1985). A review of undrained strength in direct simple shear. Soils and foundations, 25 (3), 64-72.

Randolph M. & Gourvenec S.M., (2011), Offshore Geotechnical Engineering, Spon Press/ Taylor & Francis. ISBN: 978-0-415-47744-4.

Randolph, M. F., Jewell, R. J., Stone, K. J. & Brown, T. A. (1991). Establishing a new centrifuge facility. In Proceedings of the international conference on centrifuge modelling, Centrifuge ’91, Boulder (eds H.-Y. Ko and F. G. McLean), Rotterdam, the Netherlands: Balkema, 3–9.

Randolph, M.F. (2012). Offshore design approaches and model tests for sub-failure cyclic loading of foundations. Mechanical Behaviour of Soils Under Environmentally Induced Cyclic Loads, 441-480.

Rimoy S., Jardine R.J. & Standing J.R. (2013). Displacement response to axial cycling of piles driven in sand. *Geotechnical Engineering*, 166 (GE2), 131-146

Sahdi F., Gaudin C., White D.J. & Boylan N (2014). Interpreting T-bar tests in ultra-soft clay, International Journal of Physical Modelling in Geotechnics, 14 (1), 13-19

Stewart, D. P. (1992). Lateral loading of piled bridge abutments due to embankment construction. *PhD thesis*, The University of Western Australia, Perth, Australia.

Tjelta, T.I., (2001), January. Suction piles: Their position and application today. In The Eleventh International Offshore and Polar Engineering Conference. International Society of Offshore and Polar Engineers.

Tjelta, T.I., (2015). The suction foundation technology. Frontiers in Offshore Geotechnics III, 85-93.

Tsuha C.H.C., Foray P.Y.., Jardine R.J., Yang Z.X., Silva M. & Rimoy SP. (2012). Behaviour of displacement piles in sand under cyclic axial loading. *Soils and Foundations*, 52: 393–410.

Villalobos, F.A., Byrne, B.W. & Houlsby, G.T., (2010). Model testing of suction caissons in clay subjected to vertical loading. Applied Ocean Research, 32 (4), 414-424.

Vulpe, C., Gourvenec, S.M. & Cornelius, A.F., (2017). Effect of embedment on consolidated undrained capacity of skirted circular foundations in soft clay under planar loading. Canadian Geotechnical Journal, 54 (2),158-172.

Watson P.G. & Humpheson, C. (2005). Geotechnical interpretation for the Yolla A platform. In Proc., Int. Symp. on Frontiers Offshore Geomechanics (ISFOG), 343-349, Taylor & Francis.

Yuan F., White D.J., & O'Loughlin C. (2015). The evolution of seabed stiffness during cyclic movement in a riser touchdown zone on soft clay, Geotechnique, 67 (2), 127-137

Zografou, D., Gourvenec, S., & O'Loughlin C.D. (2018a). Response of normally consolidated kaolin clay under irregular cyclic loading and comparison with predictions from the accumulation procedure (in press)

Zografou, D., Gourvenec, S., & O'Loughlin C.D. (2018b). Applicability of the strain accumulation procedure for the geotechnical foundation design of zero-radius bend triggers (submitted to Ocean Engineering – under review)

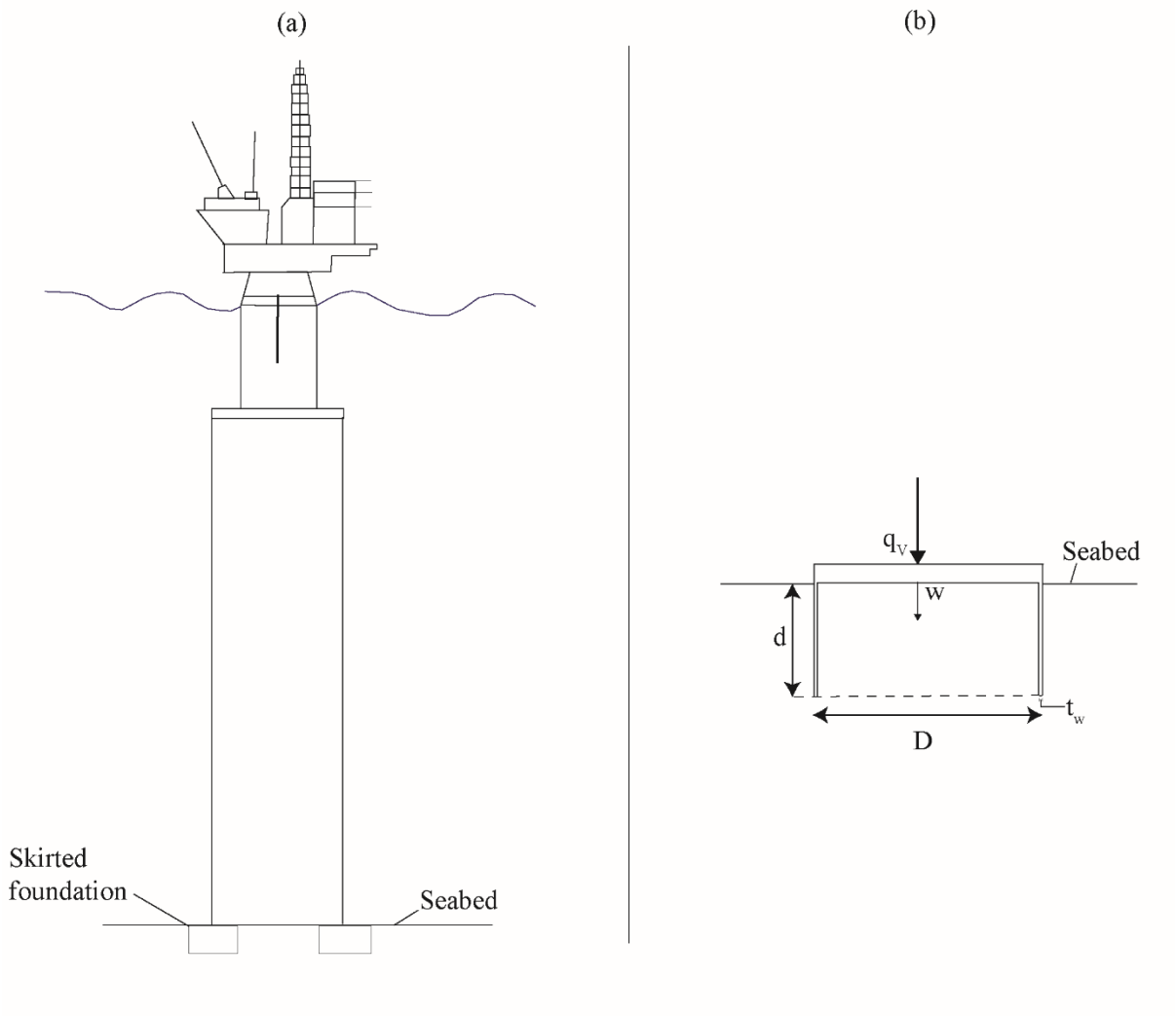

Figure 1 (a) A tension-leg platform anchored with skirted foundations and (b) skirted foundation notation (with sign convention for vertical stress, q_v, and vertical displacement, w, used in the model tests)

(a)

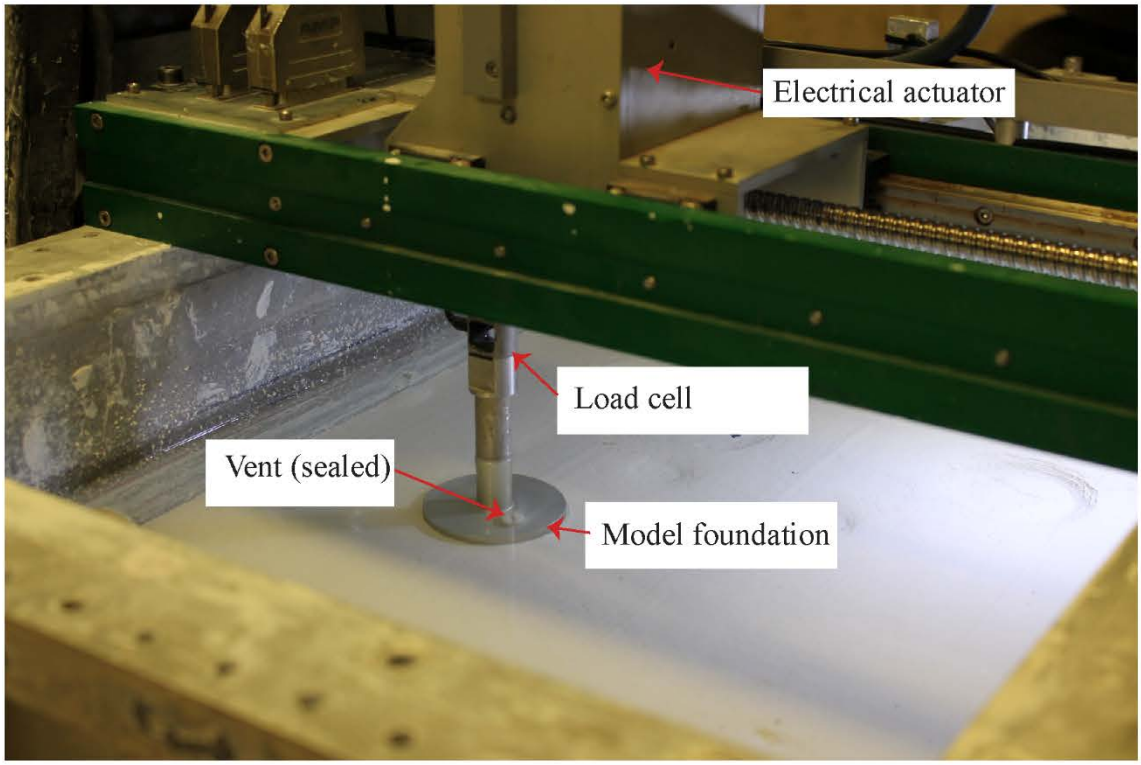
Electrical actuator
Load cell
Vent (sealed)
Model foundation

(b)

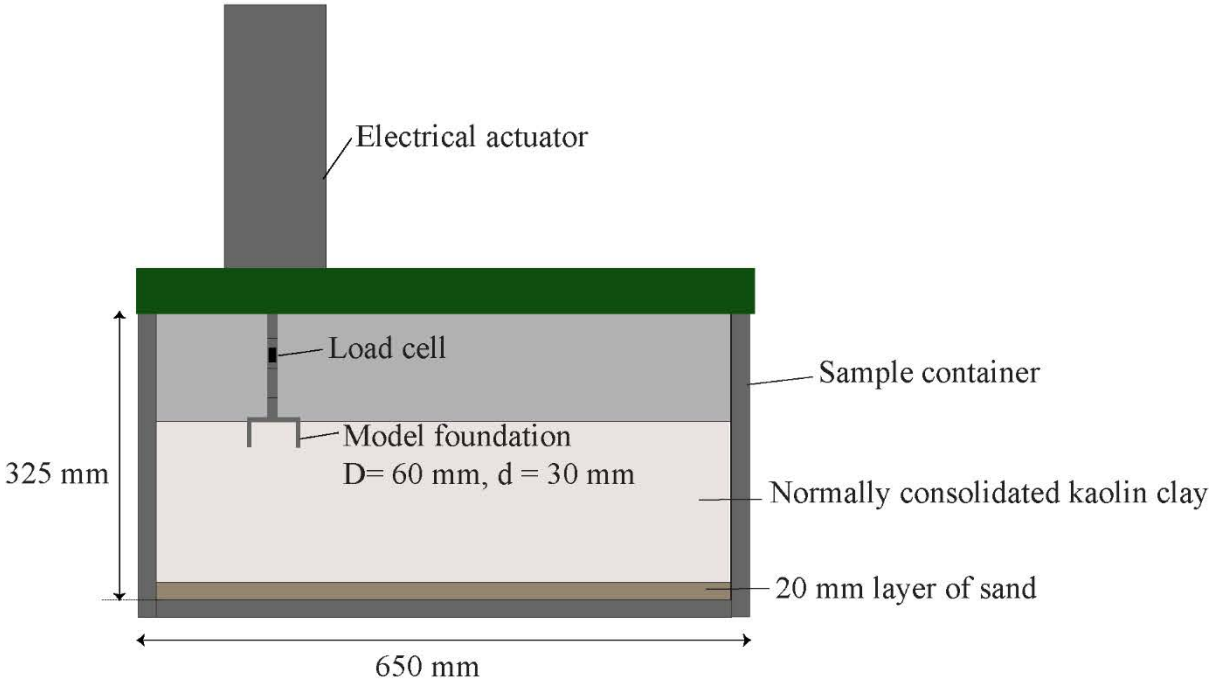
Electrical actuator
Load cell
Sample container
Model foundation
D= 60 mm, d = 30 mm
325 mm
Normally consolidated kaolin clay
20 mm layer of sand
650 mm

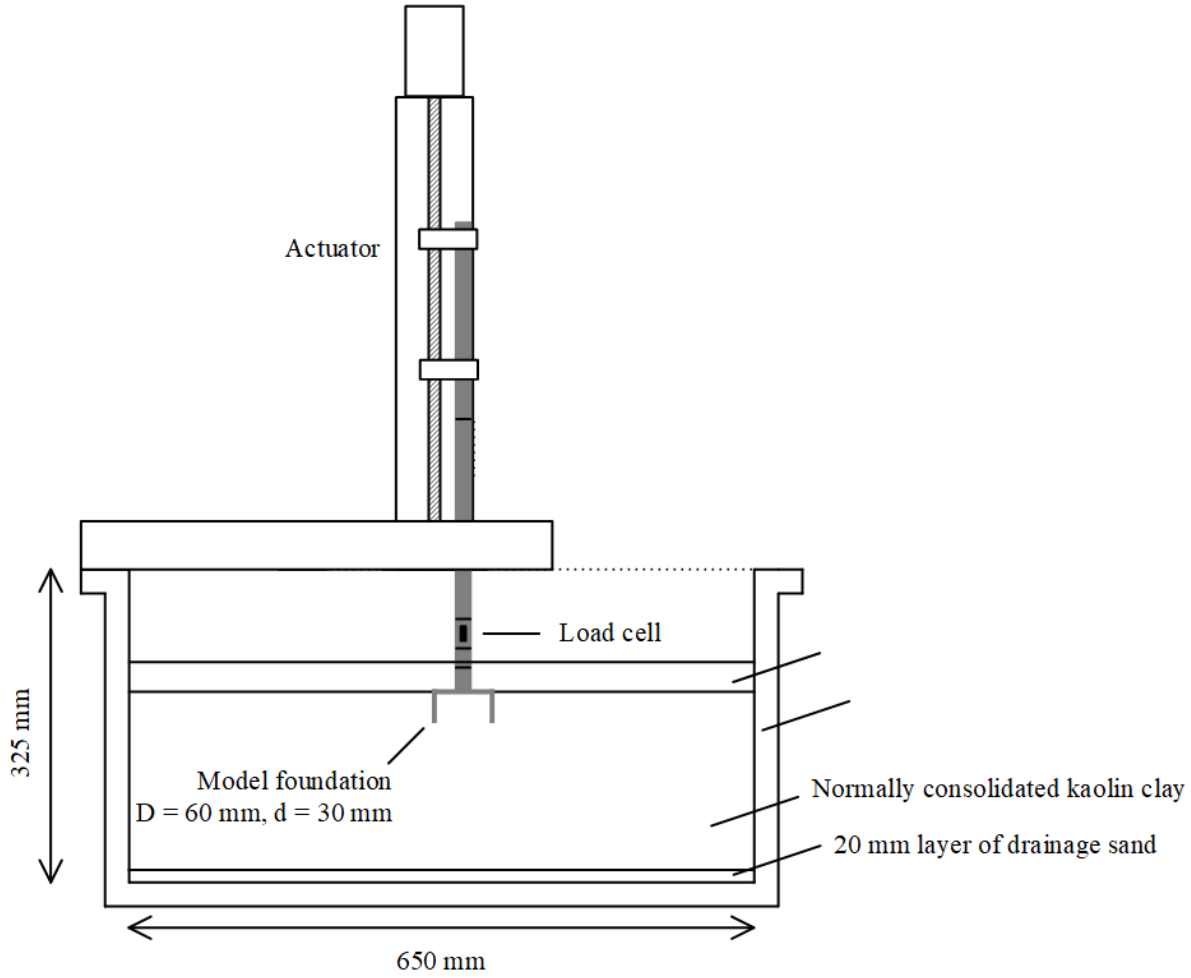

Figure 2 Experimental arrangement: (a) photograph and (b) schematic representation

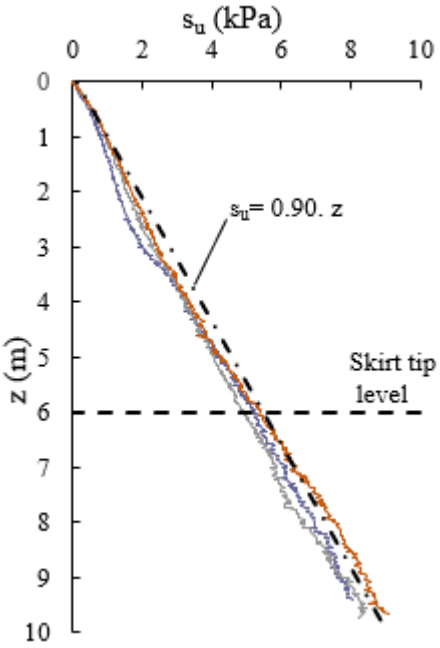

Figure 3 Undrained shear strength profile

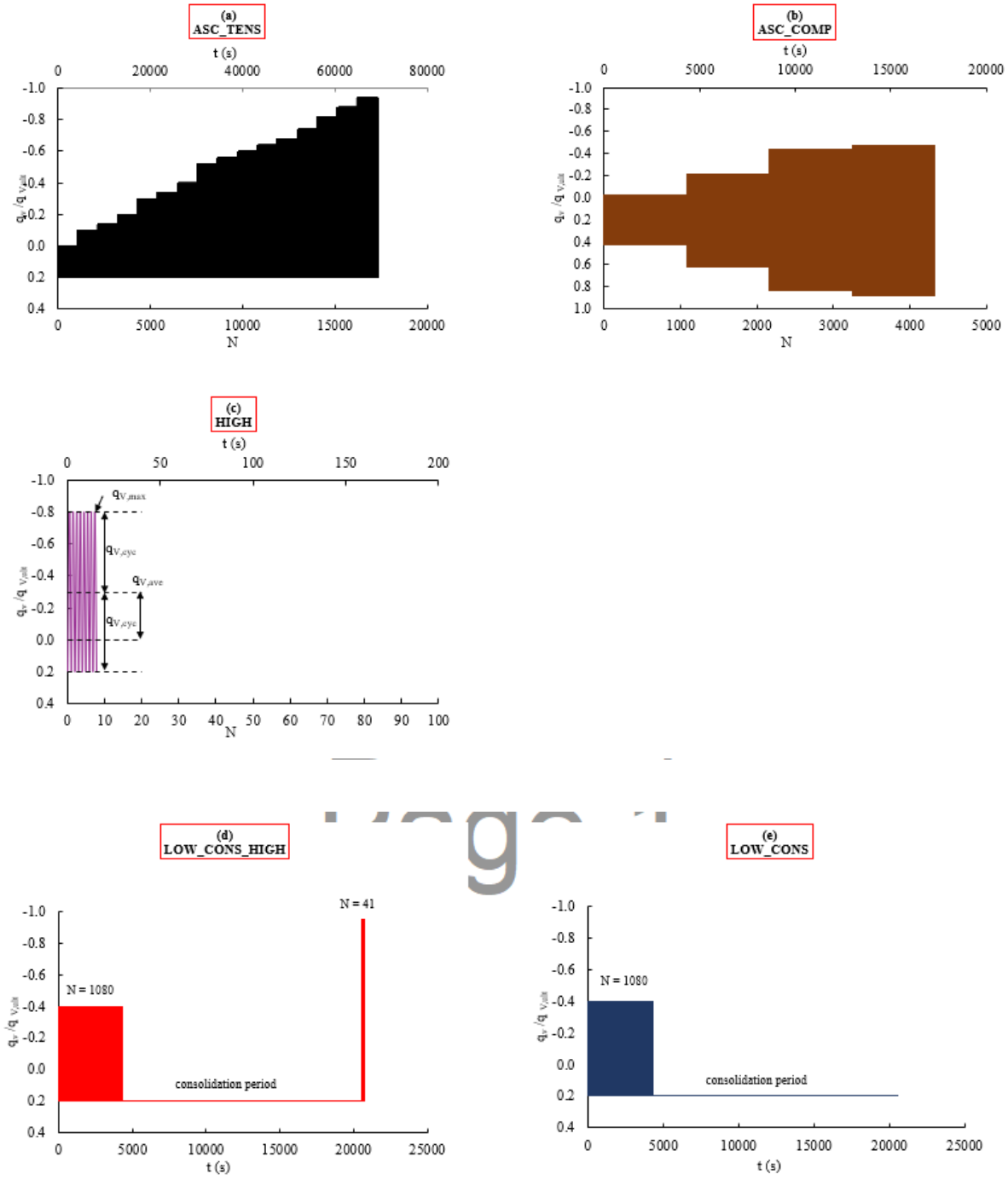

Figure 4 Schematic representation of the applied vertical cyclic stress sequences in the cyclic centrifuge tests: (a) staged cyclic test in average tension (except in the first two parcels) with parcels of uniform cyclic loading increasing in magnitude in ascending order [ASC_TENS], (b) staged cyclic test in average compression with parcels of uniform cyclic loading with magnitude increasing in ascending order [ASC_COMP], (c) uniform cyclic test in average tension and high magnitude [HIGH], (d) cyclic test (in average tension) with a parcel of uniform cyclic loading of relatively low magnitude followed by a consolidation period and a parcel of uniform cyclic loading of high magnitude [LOW_CONS_HIGH] and (e) cyclic test with a parcel of uniform cyclic loading of relatively low magnitude followed by a consolidation period [LOW_CONS]

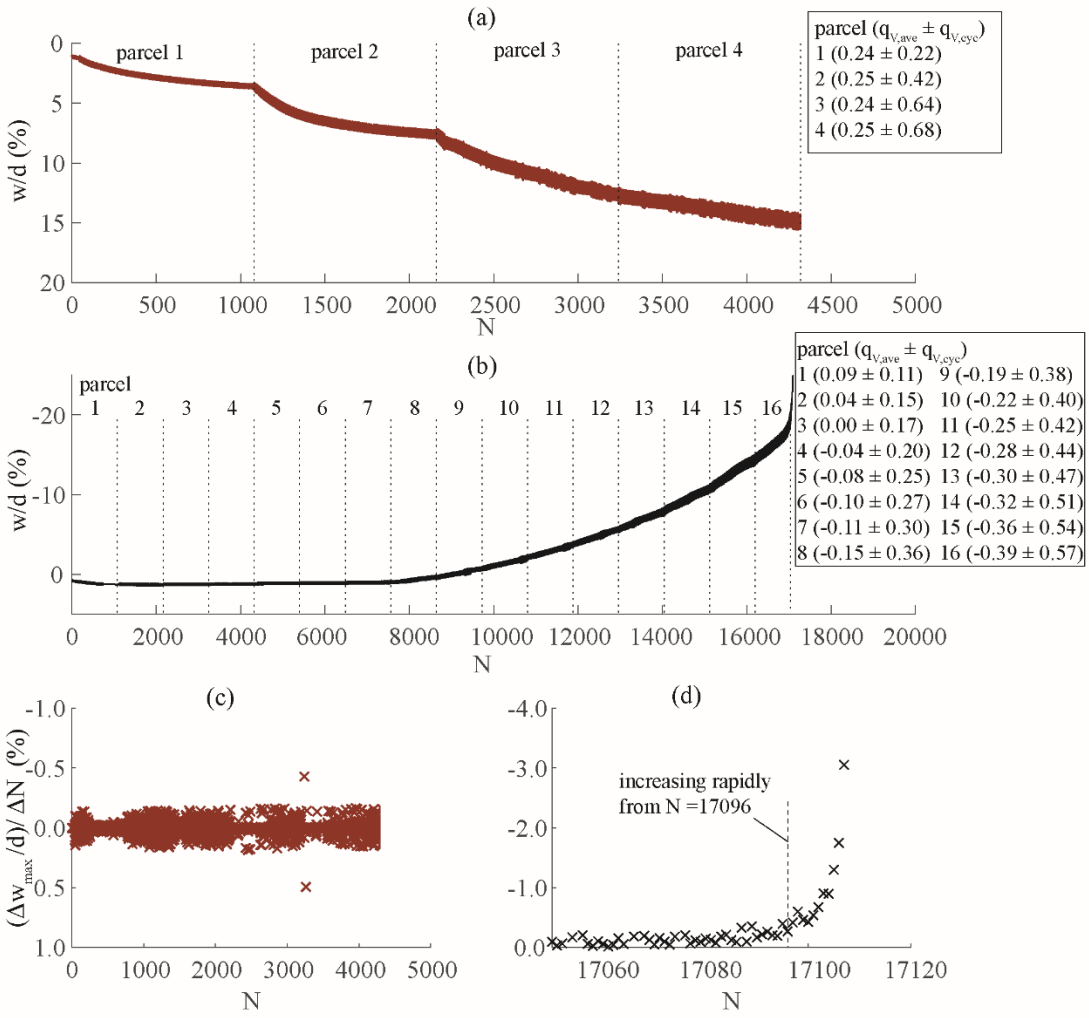

Figure 5 Vertical displacement history (vertical displacement normalised by embedment depth) during cyclic loading for (a) staged cyclic test in average compression [ASC_COMP], (b) in average tension [ASC_TENS], and c) change of vertical displacement per cycle in test ASC_COMP and d) near failure in test ASC_TENS.

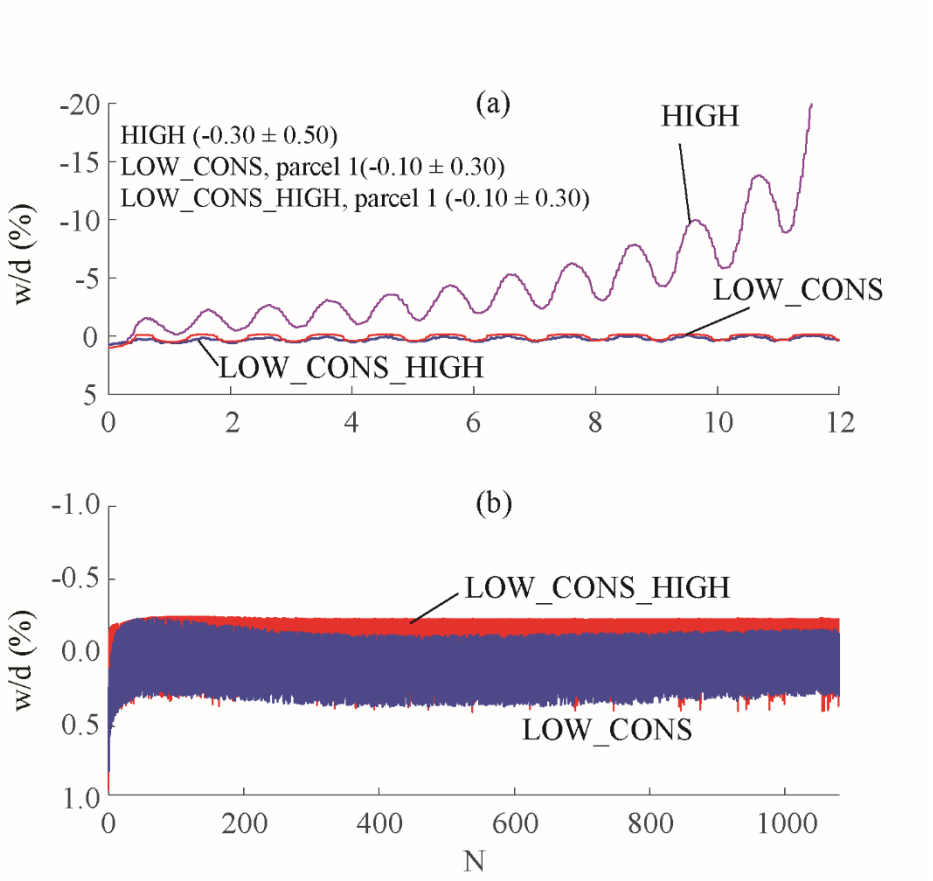

Figure 6 (a) Vertical displacement history for cyclic test with uniform high tensile vertical stress [HIGH] and tests with parcel of low tensile vertical stress [LOW_CONS, LOW_CONS_HIGH] over the first 12 cycles and (b) in a parcel of low tensile vertical stress [LOW_CONS, LOW_CONS_HIGH] over 1080 cycles.

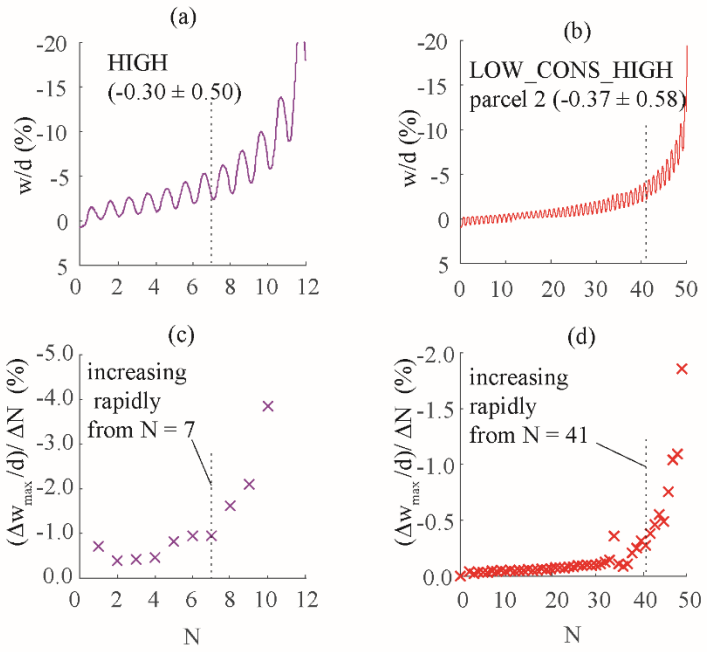

Figure 7 Vertical displacement history for (a) cyclic test with uniform high tensile vertical stress [HIGH]; N = 0 - 12, and (b) cyclic test with uniform cyclic loading in average tension followed by a consolidation period and a parcel of cyclic loading of high magnitude, in the second parcel [LOW_CON_HIGH]; N = 0 - 50, and (c, d) change in w_{max} per cycle

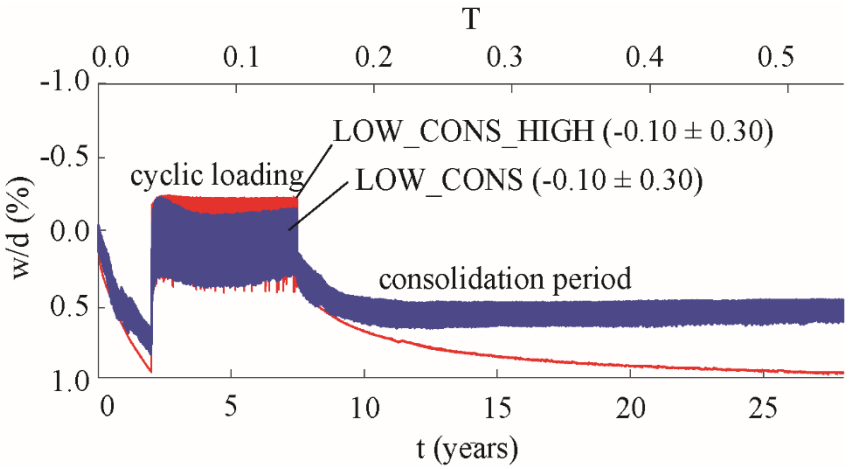

Figure 8 Vertical displacement response under a monotonic vertical stress of $0.2q_{V,ult}$ before and after cyclic loading [LOW_CONS] as a function of time, t, and as a function of dimensionless time factor, T.

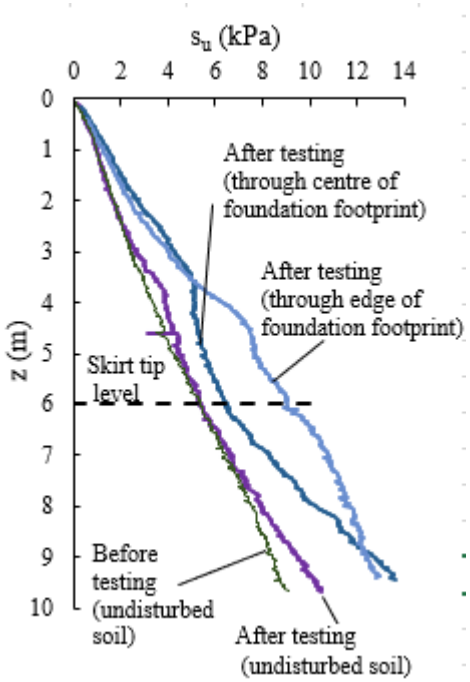

Figure 9 Profiles of undrained shear strength before and after testing

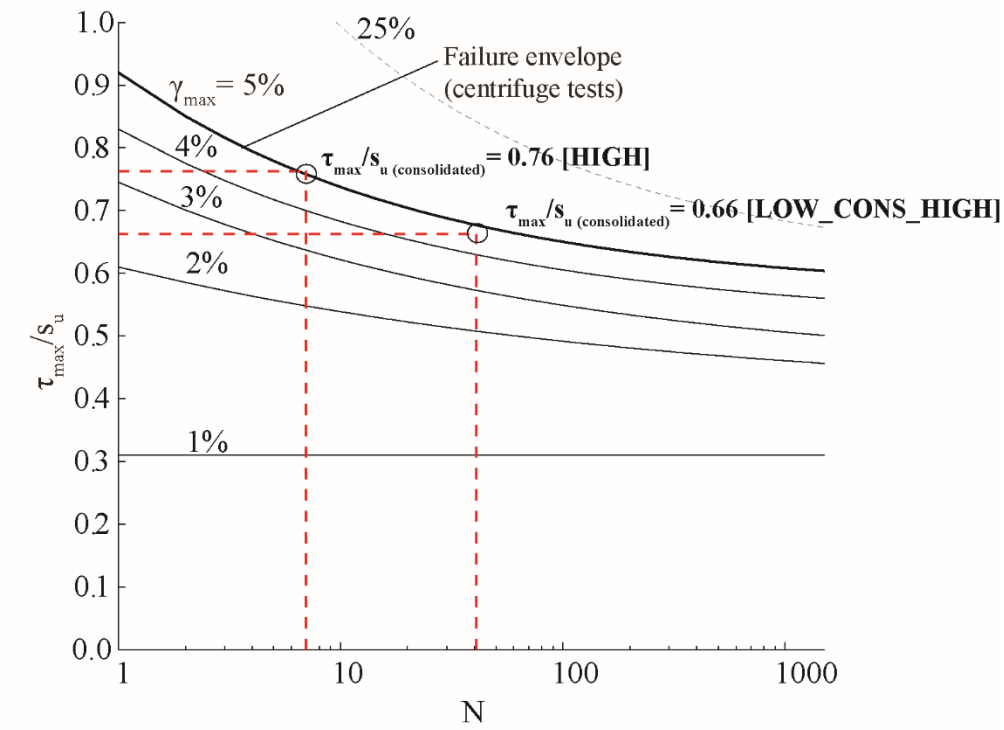

Figure 10 Final points of accumulation procedure for centrifuge test with high tensile vertical stress [HIGH] and with low-level cyclic loading followed by consolidation and then parcel with high tensile vertical stress [LOW_CONS_HIGH] on a contour diagram of maximum shear strain based on cyclic DSS tests (CSR = 1) on normally consolidated kaolin clay by Zografou et al. (2018)